# Kinetics of Peptide Binding to the Bovine 70 kDa Heat Shock Cognate Protein, a Molecular Chaperone[†]

Shigeki Takeda and David B. McKay*

*Beckman Laboratories for Structural Biology, Department of Structural Biology, Stanford University School of Medicine, Stanford, California 94305-5400*

*Received December 8, 1995; Revised Manuscript Received January 29, 1996*[⊗]

ABSTRACT: We have measured the kinetics of binding and release of a fluorescently labeled seven-residue peptide (fluorescein-FYQLALT) to recombinant bovine heat shock cognate protein (Hsc70); additionally, we have determined the effect of peptide binding on the kinetic rate constants of individual steps of the Hsc70 ATPase cycle. In the presence of MgADP, peptide binding is a two-step process; the first step results in a low-affinity peptide−Hsc70 complex ($K_d^{calcd} \approx 14$ $\mu$M), while the second step locks the peptide into a higher-affinity complex ($K_d = 4.3$ $\mu$M). In the presence of MgATP, peptide binding is a one-step process which yields a peptide−Hsc70 complex with an affinity of ∼40−50 $\mu$M. The bimolecular rates of initial peptide−Hsc70 association differ less than 2-fold in the presence of MgADP and MgATP. Peptide binding increases the rates of ATP hydrolysis and product release in the Hsc70 ATPase cycle. Taken together with earlier results, these data suggest a model for the interaction of Hsc70 with peptides in which (i) with MgATP there is significant interaction between the carboxy terminal peptide binding domain and the amino terminal ATPase domain of Hsc70 such that the effect of peptide binding is transmitted to the ATPase domain (resulting in increased rates of ATP hydrolysis and product release) and, reciprocally, the ATPase domain constrains the peptide binding domain to a low-peptide affinity conformation; and (ii) with MgADP, the peptide binding domain is less constrained by the ATPase domain, allowing capture of peptides in complexes with significantly slower "off" rates than in the presence of MgATP.

The 70 kDa heat shock proteins (Hsp70s)[1] are a family of molecular chaperones that are thought to bind partially or fully unfolded or denatured proteins *in vivo*, thereby suppressing aggregation and allowing the opportunity for proper (re)folding upon release [for review, see Pelham (1986) and Gething and Sambrook (1992)]. The bovine heat shock cognate protein (Hsc70) is a constitutively expressed representative; originally characterized as a clathrin uncoating ATPase (Schlossman et al., 1984; Chappell et al., 1986), it has been found associated with nascent polypeptides during translation (Beckmann et al., 1990) and has also been shown to facilitate transmembrane targeting of proteins (Chirico et al., 1988; Deshaies et al., 1988); it apparently manifests its molecular chaperone activity in several different contexts.

*In vitro* studies have shown that Hsp70s bind denatured proteins such as reduced, carboxymethylated lactalbumin (RCMLA) (Palleros et al., 1991), as well as some short (optimally seven or more residues) synthetic peptides (Flynn et al., 1989, 1991). Binding affinities for peptides and denatured proteins are generally weaker in the presence of MgATP than with MgADP, prompting a model in which ATP triggers release of peptides from Hsp70s.

Kinetic studies of the interaction between *Escherichia coli* DnaK protein and a fluorescently labeled 21-residue peptide derived from a mitochondrial targeting sequence demonstrated the following. (i) Peptide binding to and release from DnaK are both more rapid in the presence of MgATP than in the presence of MgADP; further, peptide affinity was higher with MgADP (peptide $K_d = 0.06$ $\mu$M) than with MgATP ($K_d = 2.2$ $\mu$M). (ii) In the presence of MgADP, peptide binding is a two-step (biphasic) process, while in the presence of MgATP, it is one-step (monophasic). (iii) Peptide binding and release is not stoichiometrically coupled to the ATPase activity (Schmid et al., 1994).

Greene and colleagues (Greene et al., 1995) and Gao and colleagues (Gao et al., 1995) have characterized the binding of both clathrin and several synthetic peptides to bovine Hsc70. They have found that both binding and release of peptides and clathrin are substantially slower in the presence of MgADP than in the presence of MgATP. With nucleotide-free Hsc70 or in the presence of nonhydrolyzable ATP analogs [5′-adenylyl $\beta,\gamma$-imidodiphosphate (AMPPNP) or $\gamma$-S-ATP], the effects are more complex. For short peptides (e.g. a 24-mer derived from cytochrome *c*), the binding rate in the presence of nonhydrolyzable analogs is similar to the rapid binding observed in the presence of MgATP, while the release rate is similar to the slower rate seen with MgADP. For clathrin, both binding and release are rapid in the presence of nonhydrolyzable ATP analogs, similar to what is observed with ATP. They have proposed that Hsc70 exists in two major conformational states; in the presence

[†] This work was supported by NIH Grant GM-39928 to D.B.M.

* Corresponding author.

[⊗] Abstract published in *Advance ACS Abstracts,* March 1, 1996.

[1] Abbreviations: Hsc70, bovine heat shock cognate protein; Hsp70, 70 kDa heat shock protein; HEPES, *N*-(2-hydroxyethyl)piperazine-*N*′-2-ethanesulfonic acid; $Mg(OAc)_2$, $Mg(CH_3COOH)_2$; FITC, fluorescein isothiocyanate; DMF, dimethylformamide; HPLC, high-performance liquid chromatography; af1, synthetic short peptide (FYQLALT); faf1, FITC-labeled af1 (fluorescein-FYQLALT); $P_i$, orthophosphate.

0006-2960/96/0435-4636$12.00/0 

of MgADP, Hsc70 is in a conformation that locks a peptide substrate onto the protein, such that peptide or clathrin release is very slow until MgADP is released and MgATP binds, inducing a second conformation that allows rapid dissociation and (re)binding of peptides.

Solution small-angle X-ray scattering studies of peptide-free recombinant bovine Hsc70 have identified two distinct conformations, one of which is observed for ADP-saturated protein and the second of which can be induced by ATP (but not by nonhydrolyzable ATP analogs) (Wilbanks et al., 1995). The kinetics of the transitions between these states under single ATPase cycle conditions reveal that the transition to the ATP-induced conformation results from ATP binding [in agreement with the interpretation of results reported earlier by Palleros et al. (1993) using different experimental methods], while the reverse transition to the ADP-associated conformation is predicated on release of the hydrolysis product ($P_i$ or ADP; the kinetic data do not discriminate which product induces the change).

We have now examined the kinetics of binding and release of a fluorescein-labeled seven-residue peptide (as monitored by the change of emission yield of the fluorophore resulting from peptide binding with Hsc70) under conditions which initially stabilize Hsc70 in each of these conformations (i.e. in the presence of a large molar excess of either ADP or ATP). We find that, in the presence of MgATP, peptide binding is monophasic, while with MgADP, it is biphasic. The data presented below provide direct support for a model in which Hsc70 in its ADP state "locks onto" or captures peptides [as proposed by Greene et al. (1995)] in a second step after initial peptide binding and that ATP inhibits the Hsc70 "peptide capture" step.

## MATERIALS AND METHODS

*Proteins and Other Reagents.* Recombinant bovine Hsc70 was expressed and purified as described previously (O'Brien & McKay, 1993; Wilbanks et al., 1994); oligomeric and aggregated protein was removed by gel filtration using a Superdex-75 column (Pharmacia, Uppsala, Sweden). Nucleotide was removed from purified Hsc70 prior to experiments with a charcoal treatment described previously (Ha & McKay, 1994). The protein concentration was determined from optical absorbance at 280 nm using the computed extinction coefficient, $3.08 \times 10^4$ $M^{-1}$ $cm^{-1}$ (Ha & McKay, 1994). [$\alpha$-$^{32}$P]ATP and [$\gamma$-$^{32}$P]ATP were purchased from Amersham. [$\alpha$-$^{32}$P]ADP was prepared as described previously (Ha & McKay, 1994).

*Peptide Synthesis, Labeling, and Purification.* A seven-residue peptide with the sequence FYQLALT (hereafter referred to as af1) was synthesized from *tert*-butyloxycarbonyl-protected amino acids using solid phase methods, and composition of the peptide was confirmed with amino acid analysis, in a local facility (PAN facility, Stanford University). The crude peptide was purified by reverse phase HPLC (model 501, Waters, Franklin, MA) on a $C_{18}$ column (250 mm $\times$ 6 mm, Alltech, Deerfield, IL); chromatographic conditions were as follows: gradient of acetonitrile, 10 to 50%, in the presence of 0.1% trifluoroacetic acid. To label the peptide with fluorescein at the amino terminus, fluorescein isothiocyanate (FITC) (Molecular Probes, Eugene, OR) was dissolved at a concentration of 10 mg/mL in dimethylformamide (DMF), 400 $\mu$L of the FITC solution was mixed with 400 $\mu$L of a solution containing 5 mg of peptide in 50% DMF and 125 mM borate buffer (pH 9.0), and the reaction was allowed to proceed for 10 h at room temperature (20−22 °C) (the fluoresceinated peptide is hereafter referred to as faf1). To stop the reaction, 150 $\mu$L of 1 M Tris-HCl (pH 8.8) was added. Peptide was separated from excess FITC on Sephadex G-25 (Sigma, St. Louis, MO) pre-equilibrated with 30% dimethylformamide. The labeled peptide, faf1, was further purified by HPLC ($C_{18}$ reversed phase column, 0 to 70% gradient of acetonitrile in the presence of 0.1% trifluoroacetic acid), lyophilized to remove organic solvents, and dissolved in water prior to use. The concentration of faf1 was determined using an extinction coefficient of $7.5 \times 10^4$ $M^{-1}$ $cm^{-1}$ at $\lambda = 493$ nm and pH 7.4 (Carilli et al., 1982; Bernhardt et al., 1983). The labeled peptide, faf1, was used both in binding assays and also in assays of the effect of peptide binding on the ATPase activity of Hsc70 because of lower solubility of the nonlabeled peptide af1.

*Measurement of Hsc70−Peptide Binding by Gel Filtration.* Hsc70, at four different concentrations ranging from 3.8 to 24 $\mu$M, was incubated with faf1 at concentrations ranging from 10 to 90 $\mu$M in 20 mM HEPES (pH 7.0), 0.1 mM ADP, 3 mM $MgCl_2$, and 150 mM KCl at 25 °C for 90 min. To assay competition between faf1 and af1 peptides, a mixture with faf1 held constant at 5 $\mu$M and af1 varied from 0 to 25 $\mu$M was used as substrate under the same conditions. Reaction mixtures were injected into an HPLC gel filtration column (SUPELCO, model TSK-G3000$SW_{XL}$, 30 cm $\times$ 7.8 mm) which was equilibrated with 20 mM HEPES (pH 7.0), 3 mM $MgCl_2$, and 200 mM KCl. The flow rate was 0.8 mL/min, and the elution volumes of Hsc70 and faf1 were about 9 and 20 mL, respectively (under these conditions, the elution volume of faf1 was greater than the column volume of 14.3 mL, while in the absence of 200 mM KCl, the peptide eluted much earlier; we presume this is due to salt-dependent hydrophobic interaction of the peptide with the column matrix). Absorbance at 494 nm was monitored with a spectrophotometer (model 481, Waters, Franklin, MA), and the relative amounts of bound and free faf1 were calculated from integrated peak areas using Baseline 810 V3.10 software (Waters, Franklin, MA). To check the effect of flow rate on integrated peak areas, chromatography was tried at rates ranging from 0.3 to 1.0 mL/min; over this range of flow rates, the variation in the amount of bound peptide, calculated as described above, was less than 10%.

*Measurement of Kinetics of Change in Fluorescence of Fluorescein-Labeled Peptide upon Binding and Release by Hsc70.* The kinetics of the change of fluorescence of the faf1 peptide resulting from binding and dissociation from Hsc70 were measured at 25 °C with a BioDX17MV Sequential Stopped-Flow ASVD Spectrofluorimeter (Applied Photophysics Ltd., Leatherhead, U.K.) equipped with a 150 W xenon arc lamp for rapid reaction (<1000 s). An excitation wavelength of 494 nm (band-pass of 1 nm) was used. Association experiments were initiated by mixing 125 $\mu$L of Hsc70, with concentration ranging from 2 to 35 $\mu$M, with 25 $\mu$L of 1.4 $\mu$M faf1, 3 mM ATP, or ADP, giving a final nucleotide concentration of 0.5 mM. To measure the dissociation rates, 50 $\mu$L of 33.4 $\mu$M Hsc70, 3.0 $\mu$M faf1 and 50 $\mu$L of 85 $\mu$M af1, 1 mM ATP or ADP were mixed. Every solution included 20 mM HEPES (pH 7.0), 150 mM KCl, and 3 mM $MgCl_2$ and was preincubated for 90 min at

25 °C. The dead time of the stopped-flow instrument was 2 ms (Tonomura et al., 1978) which was less than 0.2% of the half-time of the fastest reaction in our experiment. From previous measurements, we expect nucleotide binding to be rapid compared to the peptide−protein binding reaction; nucleotide binding is 90% complete in 40 ms under the conditions of our experiments (Ha & McKay 1994).

For observation of slow peptide−Hsc70 interaction in the presence of ADP (over the time span 0−6000 s), an SLM8000 Spectrofluorimeter (SLM Amico, Urbana, IL) was also used with an excitation wavelength of 494 nm (band-pass of 4 nm) and an emission wavelength of 510 nm (band-pass of 8 nm). Hsc70 and faf1 were preincubated at 25 °C for 90 min to form a peptide−protein complex, and the reaction was initiated by addition of af1 to the solution. The final reaction conditions were as follows: 2.6 $\mu$M Hsc70, 0.24 $\mu$M faf1, 17 $\mu$M af1, 0.5 mM ADP, 20 mM HEPES (pH 7.0), 150 mM KCl, and 3 mM $Mg(OAc)_2$ for the dissociation reaction; from 1.7 to 27 $\mu$M Hsc70, 0.24 $\mu$M faf1, 0.5 mM ADP, 20 mM HEPES (pH 7.0), 150 mM KCl, and 3 mM $Mg(OAc)_2$ for the association reaction. The time required for manual mixing was less than 15 s. Pulse−chase experiments were carried out under identical buffer conditions. Parameters were selected by simulation of the binding reaction with the program package Kinsim (Washington University; Barshop et al., 1983), using specific models for peptide binding and rate constants determined by experiment (discussed in Results). The conditions used were as follows 400 $\mu$L of 2 $\mu$M Hsc70 was mixed with 400 $\mu$L of 2 $\mu$M faf1 at 25 °C, and after 100 s, 800 $\mu$L of 2, 10, or 20 $\mu$M unlabeled af1 was added and the fluorescence change was monitored as a function of time.

Kinetic data were analyzed with software supplied with the stopped-flow instrument by the manufacturer, Applied Photophysics, with KleidaGraph (Synergy Software, Reading, PA), and with programs written by the authors. In the case of peptide binding in the presence of ADP, the time dependence of the fluorescence change was biphasic with rate constants of the two phases differing by less than 1 order of magnitude. To extract two rate constants from the fluorescence data, the rate constant of the slow phase of the reaction was first determined with data measured on a conventional fluorometer in the following manner. After subtraction of the asymptotic value ($t \rightarrow \infty$) of the fluorescence, the fluorescence change versus time was fit with a single exponential using data for times greater than 200 s for Hsc70 concentrations less than or equal to 3.4 $\mu$M and for times greater than 150 s for higher protein concentrations. Then, the rate constant of the rapid phase was determined from stopped-flow data. Using the rate constant for the slow phase determined as described above, an expression of the form $A_{slow} \exp(-k_{slow}t) + B$ (where $A$ and $B$ are adjustable parameters) was first fit to the stopped-flow data for $t >$ 200 s for [Hsc70] $\leq$ 3.4 $\mu$M and for $t >$ 150 s for [Hsc70] $>$ 3.4 $\mu$M, thereby determining the amplitude of the slow phase and the asymptotic value of the fluorescence change. The contributions of the asymptotic value and slow the phase were calculated and subtracted from the fluorescence change for times less than 30 s, and the remaining fluorescence was fit with an expression of the form $A_{rapid} \exp(-k_{rapid}t)$. Under the conditions of the experiment, the $\tau_{1/2}$ of the rapid phase ranged 12 to 23 s, so only the first 1.2−2.5 half-lives were used to determine the rate constant of the rapid phase after subtraction of the base line and the contribution of the slower phase, and only data for times at least 6 times greater than $\tau_{1/2}$ of the first phase were used to determine the amplitude of the second, slower phase.

*Measurement of Kinetics of Steps in the ATPase Cycle.* The rate constants of nucleotide binding and release, ATP hydrolysis, and $P_i$ release were determined for Hsc70 in both the presence and absence of peptide faf1, in 20 mM HEPES (pH 7.0), 150 mM KCl, and 3 mM $Mg(OAc)_2$ at 25 °C, using methods reported previously (Ha & McKay, 1994). For experiments in the presence of peptide, we mixed faf1 and Hsc70 and incubated then at 25 °C for 90 min prior to start the reaction to preform the peptide−protein complex. The association and dissociation rate constants of nucleotides (both ATP and ADP) with Hsc70 were determined with a filter binding assay using 1 nM [$\alpha$-$^{32}$P]ATP or ADP and Hsc70 over a concentration range of 20 to 160 nM. The peptide dependence of the enhancement of the ATP hydrolysis rate was determined under single turnover conditions with 10 nM [$\alpha$-$^{32}$P]ATP, 3 $\mu$M Hsc70, and faf1 ranging from 0 to 150 $\mu$M. Comparison of the ATP hydrolysis rates with and without peptide was done with 10 nM [$\alpha$-$^{32}$P]ATP, in the presence or absence of 50 $\mu$M faf1, with Hsc70 ranging from 0.05 to 4 $\mu$M. Nucleotides were separated by thin-layer chromatography (TLC) on poly(ethyleneimine)−cellulose in 0.5 M LiCl and 1 M formic acid (DeLuca-Flaherty & McKay, 1990; O'Brien & McKay, 1993), and [$\alpha$-$^{32}$P]-nucleotide was quantitated with a phosphorImager system (Molecular Dynamics, Sunnyvale, CA). Dissociation rates for $P_i$, a hydrolysis product, were determined by measuring the rate of release of radioactive label when [$\gamma$-$^{32}$P]ATP was used as the substrate, using a filter binding assay under single turnover conditions. The concentration of ATP was held constant at 10 nM, and that of Hsc70 was varied from 1.5 to 6 $\mu$M. Since ATP binding is rapid compared to hydrolysis and product release under these conditions, values of the $P_i$ off rate were computed by fitting a function with two exponential terms, one of which contained the measured ATP hydrolysis rate, to the time dependence of the loss of radioactive label from the Hsc70 complex. All kinetic data were analyzed with KleidaGraph. For a more detailed description of these methods, see Ha and McKay (1994).

## RESULTS

*Binding Constant of the faf1−Hsc70 Complex in the Presence of ADP, Measured by Gel Filtration.* First, binding of faf1 to Hsc70 in the presence of ADP was characterized by gel filtration as described in Experimental Procedures. At the concentrations employed (3.8 $\mu$M $\leq$ [Hsc70] $\leq$ 24 $\mu$M and 10 $\mu$M $\leq$ [faf1] $\leq$ 90 $\mu$M), binding reached equilibrium within the 30 min incubation period. Gel filtration, monitored at the absorbance maximum of the fluorophore, then yielded two peaks, the first of which was faf1 tightly bound to Hsc70 and the second of which was free peptide. Binding was measured at four different concentrations of Hsc70 and over a range of peptide for which 20−90% of the Hsc70 had peptide bound. Scatchard analysis of the binding data (Figure 1) yielded estimates for the faf1 dissociation constant ($K_d$) for each protein concentration, the average of which was 4.3 $\pm$ 0.9 $\mu$M. Further, the intercepts on the abcissa of the Scatchard plots demonstrate a 1:1 complex of peptide and protein; for example, in

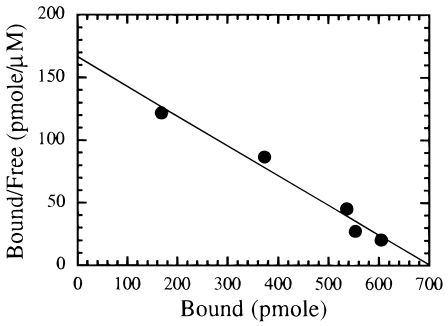


FIGURE 1: Representative Scatchard plot of gel filtration data for binding of faf1 to Hsc70. A reaction mixture with 20 $\mu$M Hsc70, faf1 ranging from 10 to 90 $\mu$M, 20 mM HEPES (pH 7.0), 0.1 mM ADP, 3 mM $MgCl_2$, and 150 mM KCl was incubated at 25 °C for 90 min. The protein solution (700 pmol of Hsc70) was then injected into a TSK-G3000$SW_{XL}$ (30 cm × 7.8 mm) HPLC column which had been pre-equilibrated with 20 mM HEPES (pH 7.0), 3 mM $MgCl_2$, and 200 mM KCl. Bound and free peptide were monitored as described in Materials and Methods.

Figure 1, the intercept has a value of 703 pmol, while 700 pmol of Hsc70 was used.

The dissociation constant of the unlabeled peptide, af1, was measured by competition with 5 $\mu$M faf1 for Hsc70 in the gel filtration assay. The concentration at which af1 inhibited faf1 binding under these conditions by 50% ($IC_{50}$) was determined from a Hill plot. The $K_i$ for af1 was then computed from the relation (Cheng & Prusoff, 1973)

$$K_i = \frac{IC_{50}}{1 + [faf1]/K_d} \quad (1)$$

The $K_i$ value of 5 $\mu$M for af1 is approximately equal to the $K_d$ value of 4 $\mu$M for faf1, demonstrating that the fluorophore does not substantially alter the equilibrium binding affinity of the peptide. This value is also consistent with reported estimates of the affinity of this peptide for Hsc70 (Fourie et al., 1994; Takenaka et al., 1995).

*Kinetics of Binding and Release of faf1 by Hsc70 in the Presence of MgADP*. When faf1 binds Hsc70, the fluorescence of the fluorescein moiety is quenched about 50%, while the maximum of the emission wavelength remains unchanged (data not shown). We have followed the kinetics of the change in fluorescence in order to monitor the kinetics of peptide binding and release. When faf1 is mixed with Hsc70 in the presence of ADP, the fluorescence decay curve is biphasic (Figure 2a). The data for the change of fluorescence versus time have been analyzed with two exponential terms as described in Experimental Procedures. The rate constant of the rapid phase shows a monotonically increasing dependence on [Hsc70], while the rate constant of the slower phase rises toward a plateau at the higher protein concentrations (Figure 2c). One explanation for biphasic kinetics could be that peptide binding by Hsc70 in the presence of ADP is a two-step process:

Scheme 1

$$E + P \underset{k_{-1}}{\overset{k_{+1}}{\rightleftharpoons}} E{-}P \underset{k_{-2}}{\overset{k_{+2}}{\rightleftharpoons}} (E{-}P)^*$$

where E represents Hsc70 and P represents peptide. In this scheme, the observed rate constants of the change in fluorescence that monitors peptide binding are roots of an equation $x^2 + bx + c = 0$, where $b = k_{+1}[Hsc70] + k_{-1} + k_{+2} + k_{-2}$ and $c = k_{+1}[Hsc70](k_{+2} + k_{-2}) + k_{-1}k_{-2}$ (Johnson, 1986). If the faster rate constant is designated $\lambda_1$ and the slower is called $\lambda_2$, then

$$\lambda_1 + \lambda_2 = b = k_{+1}[Hsc70] + k_{-1} + k_{+2} + k_{-2} \quad (2)$$

$$\lambda_1\lambda_2 = c = k_{+1}(k_{+2} + k_{-2})[Hsc70] + k_{-1}k_{-2} \quad (3)$$

The dependence of $\lambda_1 + \lambda_2$ and $\lambda_1\lambda_2$ on [Hsc70] is linear (Figure 2d,e); the slope of the line gives $k_{+1}$ and $k_{+1}(k_{+2} + k_{-2})$ equal to $(1.21 \pm 0.06) \times 10^3$ $M^{-1}$ $s^{-1}$and $(2.0 \pm 0.1) \times 10$ $M^{-1}$ $s^{-2}$, and the $y$ intercept gives $k_{-1} + k_{+2} + k_{-2}$ and $k_{-1}k_{-2}$ equal to $(3.4 \pm 0.8) \times 10^{-2}$ $s^{-1}$ and $(6.5 \pm 1.4) \times 10^{-5}$ $s^{-2}$, respectively. This gives four constants derived from experiment that relate four variables, from which we can calculate the values for $k_{-1} = (1.7 \pm 0.14) \times 10^{-2}$ $s^{-1}$, $k_{+2} = (1.3 \pm 0.15) \times 10^{-2}$ $s^{-1}$, and $k_{-2} = (3.8 \pm 0.8) \times 10^{-3}$ $s^{-1}$.

An alternative explanation for the observed biphasic kinetics could be that the peptide binds Hsc70 in two different manners:

Scheme 2

$$E{-}P \underset{k_{-1}}{\overset{k_{+1}}{\rightleftharpoons}} E + P \underset{k_{-2}}{\overset{k_{+2}}{\rightleftharpoons}} (E{-}P)^*$$

In such a scheme, either Hsc70 could switch between two different peptide binding conformations in the presence of MgADP or the peptide could bind in two different ways, to give two distinct complexes, E−P and (E−P)*. Interconversion between the two would require dissociation and rebinding of peptide. This scheme can also be parameterized by two rate constants, given by

$$\lambda_1 + \lambda_2 = (k_{+1} + k_{+2})[Hsc70] + k_{-1} + k_{-2} \quad (4)$$

$$\lambda_1\lambda_2 = (k_{+1}k_{-2} + k_{-1}k_{+2})[Hsc70] + k_{-1}k_{-2} \quad (5)$$

Approximate values derived from the kinetic data for these rate constants are as follows: $k_{+1} = 6 \times 10^2$ $M^{-1}$ $s^{-1}$, $k_{+2} = 3 \times 10^2$ $M^{-1}$ $s^{-1}$, $k_{-1} = 2.9 \times 10^{-2}$ $s^{-1}$, and $k_{-2} = 2.0 \times 10^{-2}$ $s^{-1}$. Then, computed values for the weaker and tighter binding constants are $K_1 = 50$ $\mu$M and $K_2 = 7$ $\mu$M.

To distinguish between these two alternative schemes, we carried out pulse-chase experiments in which Hsc70 was first mixed with faf1; then, after a time delay, unlabeled af1 peptide was added and the fluorescence versus time was monitored. Simulation of anticipated results for the two different cases with the program package Kinsim, using the rate constants enumerated above, led to the choice of experimental conditions. A mixture including stoichiometric amounts of protein and peptide (1 $\mu$M Hsc70 and 1 $\mu$M faf1) was mixed and allowed to incubate at 25 °C for 100 s; then, an equal volume of unlabeled af1 (2, 10, or 20 $\mu$M) was added, and the fluorescence change was monitored as a function of time. The results for the intermediate case of 5 $\mu$M final af1 concentration are shown in Figure 2f, along with simulated fluorescence curves for the two different schemes. Results for the other two concentrations were qualitatively similar; the observed fluorescence change agreed well with the simulation for the first scheme and did

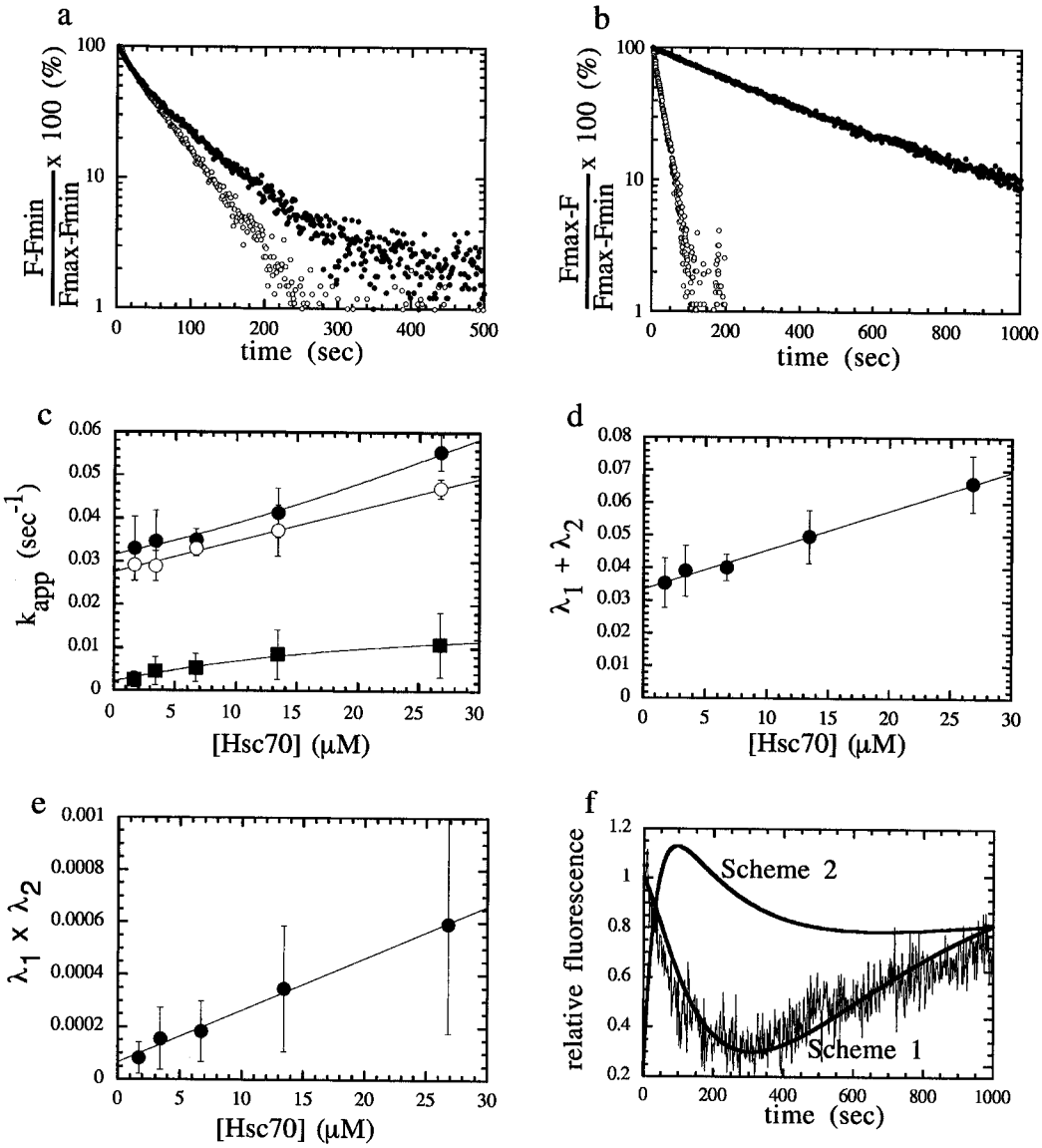


FIGURE 2: Kinetics of peptide binding and release, monitored by fluorescence. (a) Hsc70−faf1 association monitored at 25 °C as described in Materials and Methods with stopped-flow instrumentation. The conditions were as follows: 16.7 $\mu$M Hsc70, 0.23 $\mu$M faf1, 20 mM HEPES (pH 7.0), 3 mM $MgCl_2$, and 150 mM KCl, with either 0.5 mM ADP (●) or 0.5 mM ATP (○). (b) Hsc70−faf1 dissociation. Buffer and ionic conditions were essentially the same as in part a; a mixture of 2.6 $\mu$M Hsc70 and 0.24 $\mu$M faf1 was incubated at 25 °C for 90 min, and then unlabeled af1 was added to a final concentration of 17 $\mu$M at time zero, with either 0.5 mM ADP (●, measured by conventional fluorometry after manual mixing), or 0.5 mM ATP (○, measured with stopped-flow instrumentation). (c) Apparent association rate constants versus [Hsc70] for both the rapid (●) and slow (■) phases of faf1 binding in the presence of ADP and for the single phase in the presence of ATP (○). Curves show apparent rate constants calculated from values of kinetic constants in Table 1. (d) Linear fit to the sum of the two measured rate constants versus [Hsc70] for binding in the presence of ADP. (e) Linear fit to the product of the two measured rate constants versus [Hsc70] for binding in the presence of ADP. (f) Kinetics of fluorescence change in a pulse−chase experiment. The conditions were as follows. A solution with 1 $\mu$M Hsc70 and 1 $\mu$M faf1 with 0.5 mM ADP and the same buffer conditions as in part a was incubated for 100 s; then an equal volume of 10 $\mu$M unlabeled af1 was added at time zero, and the fluorescence was monitored. Simulated results that are expected for peptide binding Schemes 1 and 2 (described in text) are shown.

not agree with the simulation for the second scheme. The pulse−chase results are consistent with Scheme 1 (sequential, two-step binding) and do not support Scheme 2 (two independent binding modes).

We also measured the apparent peptide dissociation rate constant, $k_{off}^{app}$, with conventional fluorometry and manual sample mixing by monitoring the increase in fluorescence resulting from displacement of prebound faf1 from Hsc70 after addition of a large excess of unlabeled af1 peptide (Figure 2b). The fluorescence change shows a single phase with a rate constant of $0.0021 \pm 0.0001$ s$^{-1}$. In the presence of excess unlabeled peptide, the release of labeled peptide becomes essentially irreversible, and the apparent release rate for Scheme 1 is given by

$$k_{off}^{app} = \frac{k_{-1}k_{-2}}{k_{-1} + k_{+2}} \quad (6)$$

The value of $k_{off}^{app}$ computed using the rate constants determined from the binding kinetics is $0.0022 \pm 0.0009$ s$^{-1}$, equal to the measured value, which demonstrates self-consistency of the kinetic constants. As further evidence of self-consistency, we note that the equilibrium dissociation constant for Scheme 1 is given by

$$K_d = \frac{k_{-1}k_{-2}}{k_{+1}k_{+2}} \quad (7)$$

Table 1: Kinetic Parameters for Hsc70−faf1 Peptide Binding

In the presence of MgADP

| | value | method of determination |
|---|---|---|
| | Determined Experimentally | |
| $K_d$ ($\mu$M) | $4.3 \pm 0.9$ | gel filtration |
| $k_{+1}$ ($M^{-1}$ $s^{-1}$) | $(1.21 \pm 0.06) \times 10^3$ | slope of $\lambda_1 + \lambda_2$ versus [Hsc70] |
| $k_{-1} + k_2 + k_{-2}$ ($s^{-1}$) | $0.034 \pm 0.008$ | intercept of $\lambda_1 + \lambda_2$ versus [Hsc70] |
| $k_{+1}(k_2 + k_{-2})$ ($M^{-1}$ $s^{-2}$) | $(2.0 \pm 0.1) \times 10$ | slope of $\lambda_1\lambda_2$ versus [Hsc70] |
| $k_{-1}k_{-2}$ ($s^{-2}$) | $(6.5 \pm 1.4) \times 10^{-5}$ | intercept of $\lambda_1\lambda_2$ versus [Hsc70] |
| $k_{off}^{app} = k_{-1}k_{-2}/(k_{-1} + k_2)$ ($s^{-1}$) | $0.0021 \pm 0.0001$ | dissociation |
| | Calculated | |
| $k_{-1}$ ($s^{-1}$) | $0.017 \pm 0.001$ | see text |
| $k_2$ ($s^{-1}$) | $0.013 \pm 0.002$ | see text |
| $k_{-2}$ ($s^{-1}$) | $0.0038 \pm 0.0009$ | see text |
| $K_1$ ($\mu$M) | $14.2 \pm 1.2$ | $=k_{-1}/k_1$ |
| $K_2$ | $0.29 \pm 0.08$ | $=k_{-2}/k_2$ |

In the presence of MgATP

| | value | method of determination |
|---|---|---|
| | Determined Experimentally | |
| $k_{+1}$ ($M^{-1}$ $s^{-1}$) | $(7.3 \pm 0.4) \times 10^2$ | slope of $k_{on}$ versus [Hsc70] |
| $k_{-1}$ ($s^{-1}$) | $0.027 \pm 0.0005$ | intercept of $k_{on}$ versus [Hsc70] |
| $k_{-1}$ ($s^{-1}$) | $0.037 \pm 0.0003$ | dissociation |
| | Calculated | |
| $K_1$ ($\mu$M) | $37.0 \pm 2.1$ | $=k_{-1}$(from intercept)/$k_1$ |
| $K_1$ ($\mu$M) | $50.7 \pm 2.8$ | $=k_{-1}$(from dissociation)/$k_1$ |

A value of $4.3 \pm 1.2$ $\mu$M is computed from the kinetic rate constants, which agrees with the value of $4.3 \pm 0.9$ $\mu$M determined by gel filtration. All results are summarized in Table 1.

We have noticed that, when we measure the rate of complex formation by gel filtration, it shows a single linear phase on a semilogarithmic plot, while the fluorescence decrease versus time is biphasic, with a rate of change that parallels the rate of complex formation observed by gel filtration at long times. One plausible explanation for this difference is that, if peptide binding in the presence of MgADP is a two-step process (initial weak binding, followed by formation of a tighter complex), only the peptide that is tightly bound after the second step is retained as a Hsc70−faf1 complex over the course of the gel filtration experiment; gel filtration may not trap the weaker complexes because of its relatively fast dissociation rate against the flow rate of gel filtration.

*Kinetics of Binding and Release of faf1 by Hsc70 in the Presence of MgATP*. The kinetics of the change of fluorescence of faf1 after being mixed with Hsc70 in the presence of ATP were monitored. In contrast to binding in the presence of ADP, the fluorescence decay curve resulting from peptide binding to Hsc70 with ATP present shows a straight line on a semilogarithmic plot, indicating one-step binding (Figure 2a). The first order reaction can be described with a single apparent rate constant, $k_{off}^{app}$, that has a linear dependence on [Hsc70]:

$$k_{on}^{app} = k_{on}[\text{Hsc70}] + k_{off} \quad (8)$$

From a linear fit to $k_{on}^{app}$ versus [Hsc70], we compute $(7.3 \pm 0.4) \times 10^2$ $M^{-1}$ $s^{-1}$ for $k_{on}$ from the slope and $(2.7 \pm 0.05) \times 10^{-2}$ $s^{-1}$ for $k_{off}$ from the $y$ intercept (Figure 2c).

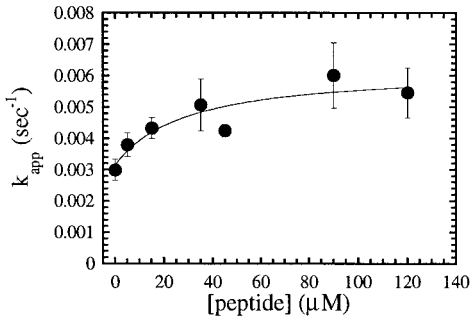


FIGURE 3: Peptide dependence of the peptide stimulation of the single turnover ATP hydrolysis rate of Hsc70. Buffer conditions were as described in Materials and Methods: 10 nM [α-$^{32}$P]ATP, 3 $\mu$M Hsc70, and faf1 ranging from 0 to 150 $\mu$M.

The dissociation rate constant in the presence of ATP was measured directly by following the change in fluorescence resulting from faf1 displacement mixing a performed complex of Hsc70−faf1 was mixed with an excess of af1 (Figure 2b). The fluorescence change due to peptide release was monophasic, with a rate constant of $(3.7 \pm 0.03) \times 10^{-2}$ $s^{-1}$, substantially more rapid than peptide release from Hsc70 in the presence of ADP. This value agrees reasonably well with the value calculated from the association data.

Using the value of $k_{on}$ determined from the association data and $k_{off}$ from either the association or dissociation data, we compute an equilibrium dissociation constant of 37 or 51 $\mu$M, respectively, for the Hsc70−faf1 complex in the presence of ATP. The results are summarized in Table 1.

*Stimulation of the ATPase Activity of Hsc70 by faf1*. Several peptides, when present in high (~1 mM) concentrations, are known to stimulate the steady state ATPase activity of monomeric recombinant bovine Hsc70 approximately 2-fold. We have determined which steps of the ATPase cycle are affected by peptide binding. First, we determined the dependence of the steady state ATPase rate and single turnover ATP hydrolysis rate on [faf1] (Figure 3). The apparent reaction rate constant, $k_{app}$, has a basal level in the absence of peptide and increases with peptide concentration in the following manner:

$$k_{app} = k'_{+2}\frac{K_M^{pep} + \beta[\text{faf1}]}{K_M^{pep} + [\text{faf1}]} \quad (9)$$

where $k'_{+2}$ is the rate of hydrolysis (the prime distinguishes rates of the ATPase reaction cycle from rates of peptide binding and release) and $\beta$ parameterizes the peptide-induced enhancement of the rate. When this function is fit to the data on the single turnover hydrolysis rate shown in Figure 3, it yields values of $29 \pm 3$ $\mu$M for $K_M^{pep}$ and 2.0 for $\beta$. This $K_M^{pep}$ value is approximately equal to the estimates of the equilibrium binding constant for the Hsc70−faf1 complex in the presence of MgATP and is substantially larger than the binding constant of ~4 $\mu$M in the presence of MgADP; the effective Michaelis constant for the peptide-dependent stimulation of the ATPase activity correlates with the peptide binding constant in the presence of MgATP. Measurements of the steady state ATPase rate gave similar results (data not shown).

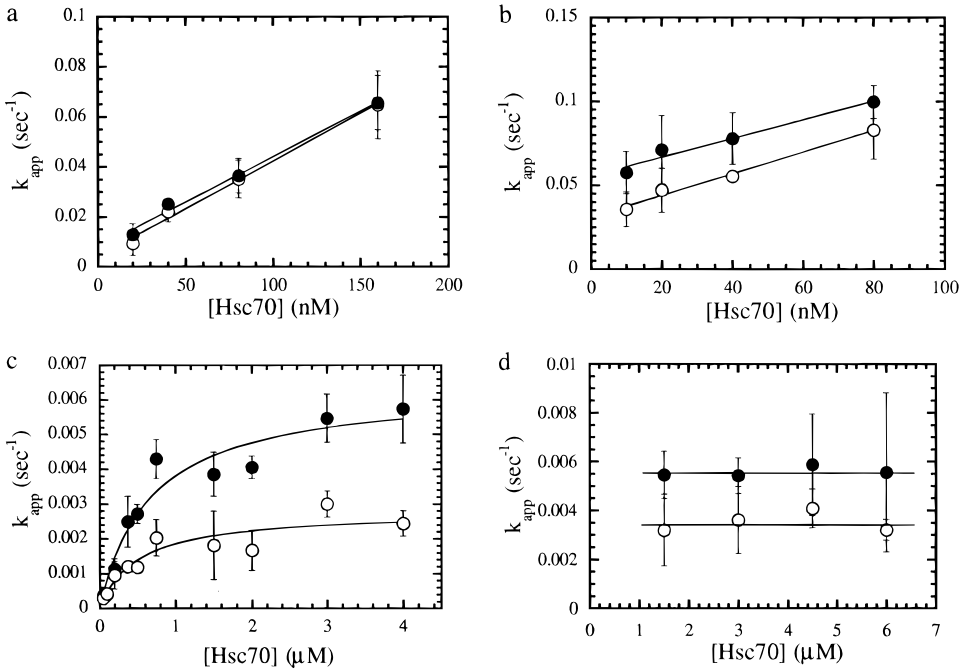


FIGURE 4: Effects of faf1 peptide on individual steps of the Hsc70 ATPase cycle. Prior to initiation of the ATPase reaction, faf1 peptide and nucleotide-free Hsc70 were mixed and incubated for 90 min at 25 °C. In panels a−d, (○) without peptide and (●) with 50 $\mu$M faf1. (a) Apparent ATP association rate versus [Hsc70]. (b) Apparent ADP association rate versus [Hsc70]. (c) Single turnover ATP hydrolysis versus [Hsc70] with 10 nM [$\alpha$-$^{32}$P]ATP and Hsc70 ranging from 0.05 to 4 $\mu$M. (d) Computed $P_i$ dissociation rate versus [Hsc70]. $P_i$ release was measured with 10 nM [$\gamma$-$^{32}$P]ATP and Hsc70 ranging from 1.5 to 6 $\mu$M; the dissociation rate was computed as described in the text.

Table 2: Effect of Peptide Binding on Kinetic Rate Constants of Individual Steps of the ATPase Cycle

| | Hsc70 | Hsc70 + 50 $\mu$M faf1 | Hsc70[a] | 44 kDa[a] |
|---|---|---|---|---|
| $k'_{+1}$ ($M^{-1}$ $s^{-1}$) | (3.82 ± 0.24) × $10^5$ | (3.62 ± 0.24) × $10^5$ | (2.69 ± 0.46) × $10^5$ | nd[b] |
| $k'_{-1}$ ($s^{-1}$) | 0.0042 (±0.0022) | 0.0079 (±0.0022) | 0.0114 (±0.0002) | nd |
| $k'_{+2}$ ($s^{-1}$) | 0.0028 (±0.0003) | 0.0064 (±0.0006) | 0.0030 (±0.0003) | 0.0135 (±0.0033) |
| $k'_{+3}$ ($s^{-1}$) | 0.0035 (±0.0010) | 0.0056 (±0.0017) | 0.0038 (±0.0010) | 0.0051 (±0.0006) |
| $k'_{+4}$ ($s^{-1}$) | 0.0310 (±0.0023) | 0.0556 (±0.0035) | 0.0288 (±0.0018) | 0.0347 (±0.0016) |
| $k'_{-4}$ ($M^{-1}$ $s^{-1}$) | (6.5 ± 0.5) × $10^5$ | (5.6 ± 0.7) × $10^5$ | (4.1 ± 0.5) × $10^5$ | nd |
| $K_m$ ($\mu$M) | 0.51 (±0.20) | 0.67 (±0.19) | 0.25 (±0.05) | 0.65 (±0.34) |

[a] Determined previously with 75 mM KCl (Ha & McKay, 1994). [b] Not determined.

Since nearly full stimulation was observed at a faf1 concentration of 50 $\mu$M, this was chosen as a pragmatic concentration for measuring kinetic parameters of individual steps of the ATPase cycle with and without peptide. The methods employed have been described in detail previously. The apparent association rates of MgATP and MgADP with Hsc70 were determined with a filter binding assay (Figure 4a,b), and the on and off rates of the nucleotide were computed from the slope and intercept, respectively, of a linear fit to the data. The binding data show that the peptide has a negligible effect on the rate of binding of either nucleotide and on the rate of release of MgATP; however, the off rate of MgADP is approximately twice as fast in the presence of peptide as in the absence.

A substantial peptide-induced change in the rate of single turnover MgATP hydrolysis was seen. $K_M^{st}$ and $k'_{+2}$ were calculated by fitting the Michaelis−Menten expression to the data (Figure 4c):

$$k_{app} = \frac{k'_{+2}[\text{Hsc70}]}{K_M^{st} + [\text{Hsc70}]} \quad (10)$$

Bound peptide increased the rate of ATP hydrolysis without significantly altering the concentration of half-maximal activity ($K_M^{st}$).

The rate of $P_i$ release was determined as described previously (Ha & McKay, 1994), by measuring the release of label from [$\gamma$-$^{32}$P]ATP and fitting the fraction of radiolabel released versus time with a function that incorporates two rate constants, one of which ($k'_{+2}$) is that of MgATP hydrolysis determined above:

$$\Phi(t) = C\frac{k'_{+2}\exp(-k'_{+3}t) - k'_{+3}\exp(-k'_{+2}t)}{k'_{+2} - k'_{+3}} \quad (11)$$

Over the Hsc70 concentration range from 1.6 to 6 $\mu$M, the computed $P_i$ release rates are independent of protein concentration (Figure 4d). The $P_i$ release rate is higher in the presence of peptide than in its absence; peptide binding accelerates both $P_i$ release and ATP hydrolysis. Results of the current study are summarized in Table 2 and are compared to earlier results (Ha & McKay, 1994).

## DISCUSSION

We have measured the kinetics of binding and release of fluoresceinated FYQLALT by Hsc70. In the presence of MgATP, binding and release are single phase and the affinity of the peptide for Hsc70 is ~40−50 $\mu$M. In the presence of MgADP, the peptide binds in two sequential steps. The

binding and release rates of the first step differ by less than 2-fold in magnitude from those measured in the presence of MgATP. From this, we infer that the initial step of peptide binding to Hsc70 is not dramatically different in the presence of either MgADP or MgATP and that what distinguishes low affinity from high affinity peptide binding is the ability of Hsc70 to undergo a second step in the presence of MgADP, resulting in a higher affinity complex with a substantially slower dissociation rate. The effect of MgATP on Hsc70 is to inhibit the second step of binding, thereby stabilizing the protein in a low peptide affinity state.

Our results can be compared to those reported by other investigators. Greene et al. (1995) have measured binding of a 24-residue cytochrome *c* peptide to both bovine Hsc70 and yeast Ssa1p using gel filtration. In the presence of MgADP, the $K_d$ values of the cytochrome *c* peptide are 7 and 2 $\mu$M for Hsc70 and Ssa1p, respectively, similar to the value of 4 $\mu$M that we find for the faf1−Hsc70 complex. In the presence of MgATP, the cytochrome *c* peptide $K_d$ values are 300 and 25 $\mu$M for Hsc70 and Ssa1p, respectively. These bracket the value of 40−50 $\mu$M we find for faf1 binding to Hsc70 with MgATP. Thus, a difference on the order of $10^1$−$10^2$-fold in $K_d$ between the low- and high-affinity complexes is seen in all cases, corresponding to a relatively modest free energy difference on the order of 1−3 kcal/mol. A difference of this magnitude was also reported for binding of a fluorescently labeled peptide to DnaK (Schmid et al., 1994), although the affinities were substantially tighter (0.06 $\mu$M in the presence of MgADP as opposed to 2−4 $\mu$M with MgATP).

Greater variation is reported for on and off rates of peptides than for their equilibrium binding constants. Of particular interest in the context of the biological functions of the Hsp70 proteins are peptide dissociation rates. For the cytochrome *c* peptide in the presence of MgADP, the dissociation rate is on the order of $10^{-4}$ $s^{-1}$ for both Hsc70 and Ssa1p, while for the faf1−Hsc70 complex, it is on the order of $10^{-3}$ $s^{-1}$ (Greene et al., 1995). Such differences may be intrinsic to the particular lengths and sequences of peptides used in the different studies. In this context, it is worth noting that clathrin binds Hsc70 with $K_d$ values of the same order as observed for shorter peptides, 3 and 12 $\mu$M in the presence of MgADP and MgATP, respectively; however, the kinetics of binding and release differ substantially from those of the shorter peptides, with the dissociation rate in the presence of MgADP being $<10^{-4}$ $s^{-1}$ (Greene et al., 1995) . The similarity in $K_d$ values may reflect similar interactions of different peptides across a peptide binding site which is thought to span about seven amino acid residues, while the variations in kinetics of binding and release may result from such factors as differences in peptide length and sequence.

Peptide binding stimulates the ATP hydrolysis and product release rates of the ATPase cycle of recombinant Hsc70 approximately 2-fold, increasing the rate constants toward the values observed for the isolated ATPase domain (Ha & McKay, 1994). More specifically, the ATP hydrolysis rate of Hsc70 is stimulated approximately 2-fold by faf1, whereas the hydrolysis rate of the ATPase fragment is approximately 4-fold higher than that of the full-length protein. Peptide binding stimulates the $P_i$ and ADP release rates to values approximately equal to those of the ATPase domain. Qualitatively, it appears that the carboxy terminal domain of Hsc70 inhibits ATP hydrolysis and product release, relative to their intrinsic rates in the ATPase domain alone, and that binding of peptide alleviates, but does not completely eliminate, the inhibition.

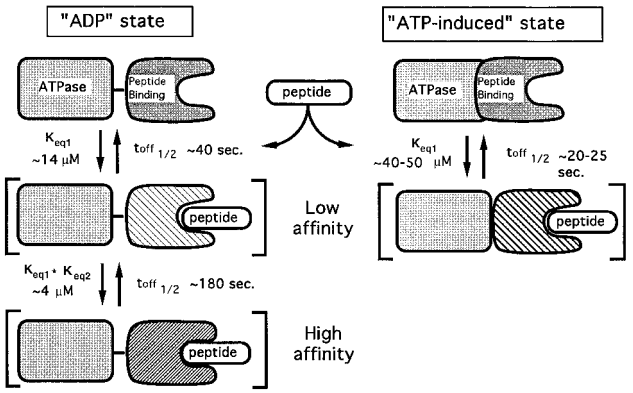


FIGURE 5: Schematic model of peptide-free and peptide-bound states of Hsc70. The amino terminal ATPase domain and carboxy terminal peptide binding domain are represented as distinct entities. The peptide-free conformations have been parameterized by solution X-ray scattering, and approximate overall dimensions are given in the references; peptide-bound conformations have not been similarly characterized and therefore are enclosed in brackets. The conformation of the peptide binding domain in the ADP form after the initial step of binding may be similar in structure to the domain with peptide bound in the ATP-induced form. Dissociation half-lives for the faf1 peptide are computed as $0.69/k_{off}$.

Solution small-angle X-ray-scattering studies have delineated two substantially different conformations for peptide-free Hsc70 (Wilbanks et al., 1995). With MgADP, the protein is relatively elongated and the peptide binding domain is likely to be relatively disengaged from the ATPase domain, while with MgATP, it is more compact and it is probable that there are significant interactions between the peptide binding and ATPase domains [for a detailed discussion, see Wilbanks et al. (1995)]. ATP binding induces the transition to the MgATP form of Hsc70, while relaxation back to the MgADP form is predicated on product ($P_i$ or ADP) release. Peptide stimulation of ATP hydrolysis and product release rates would therefore be exerted mostly, if not exclusively, on the ATP-induced state of Hsc70. The fact that binding of peptide alters the kinetic constants of the ATPase reaction implies that the effect of peptide binding to the carboxy terminal domain must be transmitted to the amino terminal ATPase domain, presumably by a (perhaps subtle) change in the overall conformation of Hsc70. These data suggest an extension of the earlier schematic model developed for peptide-free Hsc70 to incorporate the effects of peptide binding (Figure 5). In the presence of MgATP, peptide association induces a conformational change in the carboxy terminal domain of Hsc70; presumably, the interaction between the carboxy and amino terminal domains that results in stimulation of the ATPase activity also constrains the peptide binding domain in a low affinity conformation. In the presence of MgADP, the peptide binding domain would not be as constrained by the ATPase domain and could capture the peptide to form a high affinity complex in the second step of binding.

In the more general contest of molecular chaperone activity, these results are compatible with a scheme in which (i) the biological effects of chaperone activity are determined by their release rates for bound polypeptides and (ii) the adenine nucleotide serves a regulatory function. In the presence of a high intracellular ATP/ADP ratio, which would

be expected in cells under normal circumstances, Hsc70 would spend most of its time in its ATP-induced conformation and bound polypeptides or proteins would have a relatively rapid release rate. Under stress conditions or other conditions that lowered the ATP/ADP ratio, Hsc70 would spend a significant fraction of time in its ADP-bound state; bound polypeptides would have a relatively slow release rate and would be captured as Hsc70−polypeptide complexes, presumably to stabilize them against misfolding or aggregation under cellular conditions in which correct folding is disfavored.

## ACKNOWLEDGMENT

We thank Drs. Jon Goldberg and Marc Jamin for the assistance with the stopped-flow spectrofluorometer. We thank also Dr. Lubert Stryer and the Stanford University Biochemistry Department for the use of spectrofluorometers. We gratefully acknowledge Dr. Jeung-Hoi Ha for providing purified af1 peptide. We also acknowledge Drs. Sigurd M. Wilbanks and Eric Johnson for helpful discussions.

## REFERENCES

Barshop, B. A., Wrenn, R. F., & Frieden, C. (1983) *Anal. Biochem. 130*, 134−145.

Beckmann, R. P., Mizzen, L. A., & Welch, W. J. (1990) *Science 248*, 850−854.

Bernhardt, R., Ngoc Dao, H. T., Stiel, H., Schwarze, W., Friedrich, J., Janig, G., & Ruckpaul, K. (1983) *Biochim. Biophys. Acta 745*, 140−148.

Carilli, C. T., Farley, R. A., Perlman, D. M., & Cantley, L. C. (1982) *J. Biol. Chem. 257*, 5601−5606.

Chappell, T. G., Welch, W. J., Schlossman, D. M., Palter, K. B., Schlesinger, M. J., & Rothman, J. E. (1986) *Cell 45*, 3−13.

Cheng, Y., & Prusoff, W. H. (1973) *Biochem. Pharm. 22*, 3099−3108.

Chirico, W. J., Waters, M. G., & Blobel, G. (1988) *Nature 332*, 805−810.

DeLuca-Flaherty, C., & McKay, D. B. (1990) *Nucleic Acids Res. 18*, 5569−5569.

Deshaies, T. J., Koch, B. D., Werner-Washburne, M., Craig, E. A., & Schekman, R. (1988) *Nature 332*, 800−805.

Flynn, G. C., Chappell, T. G., & Rothman, J. E. (1989) *Science 245*, 385−390.

Flynn, G. C., Pohl, J., Flocco, M. T., & Rothman, J. E. (1991) *Nature 353*, 726−730.

Fourie, A. M., Sambrook, J. F., & Gething, M. J. (1994) *J. Biol. Chem. 269*, 30470−30478.

Gao, B., Eisenberg, E., & Greene, L. (1995) *Biochemistry 34*, 11882−11888.

Gething, M. J., & Sambrook, J. (1992) *Nature 355*, 33−45.

Greene, L. E., Zinner, R., Naficy, S., & Eisenberg, E. (1995) *J. Biol. Chem. 270*, 2967−2973.

Ha, J.-H., & McKay, D. B. (1994) *Biochemistry 33*, 14625−14635.

Johnson, K. A. (1986) *Methods Enzymol. 134*, 677−705.

O'Brien, M. C., & McKay, D. B. (1993) *J. Biol. Chem. 268*, 24323−24329.

Palleros, D. R., Welch, W. J., & Fink, A. L. (1991) *Proc. Natl. Acad. Sci. U.S.A. 88*, 5719−5723.

Pelham, H. R. B. (1986) *Cell 46*, 959−961.

Schlossman, D. M., Schmid, S. L., Braell, W. A., & Rothman, J. E. (1984) *J. Cell Biol. 99*, 723−733.

Schmid, D., Baici, A., Gehring, H., & Christen, P. (1994) *Science 263*, 971−973.

Takenaka, I. M., Leung, S.-M., McAndrew, S. J., Brown, J. P., & Hightower, L. E. (1995) *J. Biol. Chem. 270*, 19839−19844.

Tonomura, B., Nakatani, H., Ohnishi, M., Yamaguchi-Ito, J., & Hiromi, K. (1978) *Anal. Biochem. 84*, 370−383.

Wilbanks, S. M., DeLuca-Flaherty, C., & McKay, D. B. (1994) *J. Biol. Chem. 269*, 12893−12898.

Wilbanks, S. M., Chen, L., Tsuruta, H., Hodgson, K. O., & McKay, D. B. (1995) *Biochemistry 34*, 12095−12106.

BI952903O